Microwave spectrum of PHD: hyperfine structure

Microwave spectrum of PHD: hyperfine structure

Takashi Furuya and Shuji Saito

Research Center for Development of Far-Infrared Region, Fukui University, 3-9-1 Bunkyo, Fukui 910-8507, Japan

Abstract

The rotational spectrum of the monodeuterated PH_2 radical was studied using a source-modulated submillimeter-wave spectrometer. The PHD radical was generated in a free space absorption cell by a dc-glow discharge in a gas mixture of PH_3 and D_2. Six *a*-type and 20 *b*-type rotational transitions were observed in the frequency region of 170–670 GHz. Hyperfine structure due to the deuterium nucleus was resolved only in the rotational transitions of 1_{11}–0_{00} and 1_{10}–1_{01} and in the low F_2 components of $N = 2$–1 transitions. A total of 219 spectral lines were measured of which 145 were analyzed by least-squares methods. These yielded 34 precise molecular constants including the hyperfine coupling constants of phosphorus, hydrogen, and deuterium. The principal axes and principal values of the magnetic dipole coupling tensors of hydrogen in PH_2 and deuterium in PD_2 were derived from the observed values of PHD, PH_2 and PD_2. The principal axis of the hydrogen magnetic dipole coupling tensor in PH_2 makes an angle of 2.29° with the PH bond and its T_σ and $T_\perp$ principal values are determined to be 12.93 and −18.39 MHz, respectively.

Keywords: Free radical; PHD; Rotational spectrum; Submillimeter-wave; Hyperfine structure

1. Introduction

The hyperfine structure of a molecule reflects its bonding. The principal values of the hyperfine coupling tensor are essential to obtain a substantial picture of the nature of the bonding. However, the principal value of the tensor is not readily ascertained, when the atom is located in an off-axial position. In some cases, the off-diagonal component of the hyperfine coupling tensor could be determined due to an accidental degeneracy of interacting levels. This cannot be applied to the hyperfine structures of hydrogen and deuterium because the magnitude of their interaction is relatively small. The XH_2-type free radicals contain such atoms and the off-diagonal component of the hyperfine coupling tensor for H cannot be determined by conventional microwave spectroscopy. The NH_2 [1] and ND_2 [2] radicals were studied by microwave spectroscopy and their detailed molecular constants were precisely determined except for the off-diagonal components of the magnetic dipole tensors, T_{ab}, for H and D. Steimle et al. [3] studied the ground vibronic state of NHD with a microwave optical double resonance method and determined the T_{ab} constant for NH_2 from the MODR spectrum of NHD by considering the principal axis rotation in NH_2 and NHD. Later, their result was confirmed to be consistent with the experimentally determined value of T_{ab} for H in the microwave spectroscopic study of NHD [4]. Saito et al. [5] extended this idea and showed that the off-diagonal component of the magnetic dipole tensor can be derived from the diagonal components of the isotopic species using the assumption that the unpaired electron distribution in related atoms does not change much upon isotopic substitution. They applied this method to the case of HO_2 and DO_2, deriving the off-diagonal components of magnetic dipole coupling constants for both species from their diagonal components, and determined the principal axes and values for the hydrogen in HO_2, which clarified the relation between the HO bond and unpaired electron distribution near the related O atom.

The PH_2 radical is isovalent to NH_2. The hyperfine structure of PH_2 [6–8] and PD_2 [9] was studied by microwave spectroscopy. Endo et al. [6] first observed the pure rotational spectrum of PH_2 in the millimeter-wave

region, and analyzed it to precisely determine the detailed molecular constants. They found a large contribution of phosphorus nuclear spin–rotation interaction to the hyperfine structure. Kajita et al. [7] extended the measurements into the submillimeter-wave region up to 400 GHz and Margulès et al. [8] further extended them up to 1 THz. Accordingly they revised much of the molecular constants, particularly the higher-order centrifugal distortion effect. Hirao et al. [9] observed the microwave spectrum of PD_2. They carried out a harmonic force field analysis using centrifugal distortion constants, inertial defects and vibrational frequencies, and derived the r_z structures of PH_2 and PD_2. However, the off-diagonal component of the magnetic dipole coupling constant of H or D is not known experimentally. The monodeuterated species of PH_2, PHD, has been studied to date only by emission spectroscopy which revealed ν_2 band sequences in both ground and excited electronic states, $\tilde{X}^2B_1$ and $\tilde{A}^2A_1$ [10,11].

Similarly to NHD, one of the hydrogens in PH_2 is replaced by a deuterium atom and then the principal axis rotates by an angle of 38.74°, which yields a dipole moment along the a-axis of $0.6258\mu_b$ where μ_b is the dipole moment of the symmetric PH_2. This gives two thirds the intensity of the b-type transition to the a-type in PHD and increases the number of measurable transitions in the submillimeter-wave region. In the present study we measured a-type and b-type rotational transitions of PHD and precisely determined the molecular constants.

2. Experimental

The submillimeter-wave spectrometer previously reported [12] was used to observe spectral lines of PHD. The monodeuterated species was first generated by a hollow cathode discharge in a gas mixture of H_2 and D_2 over red phosphorus grains which were placed directly in the middle of a Pyrex-glass free-space absorption cell, as in the study of PD_2 [9]. However, the spectral line intensity was not sufficient for observations of relatively weak forbidden transitions, which are essential in the determination of all the hyperfine coupling constants. The red phosphorus grains were then replaced by PH_3. This production method gave signals two times stronger in intensity. Production conditions were optimized using a known spectral line of PH_2 [6]. The optimum conditions were 15 mTorr for partial pressures of both PH_3 and D_2 and a discharge current of 200 mA. The cell temperature was maintained at −60 to −90 °C to ensure a stable discharge.

Prior to observations of PHD spectral lines, transition frequencies were predicted from a set of molecular constants; the rotational constants were calculated from the reported r_z structure of PH_2 and PD_2 [9], centrifugal distortion constants were assumed to be those of HDS [13] and the fine and hyperfine coupling constants calculated from those of PH_2 [7] and PD_2 [9]. The predicted spectral pattern showing fine and hyperfine structures for each rotational transition was helpful in its identification because spectral lines of PH_2, PHD, and PD_2 were simultaneously present throughout the entire frequency region with similar intensity. As an example, a spectral pattern of the 1_{11}–0_{00} transition is shown in Fig. 1. When a line showing paramagnetic behavior was observed, it was necessary to check whether the source of the signal was due to PHD by stopping the flow of D_2. The b-type Q-branch transitions, 3_{21}–3_{12} and 4_{22}–4_{13}, having relatively strong intensity were initially searched for in the 300 GHz region. Four groups of congested spectral lines were detected in the range, 367–377 GHz and assigned to the two Q-branch transitions on the basis of the predicted spectral patterns. The im-

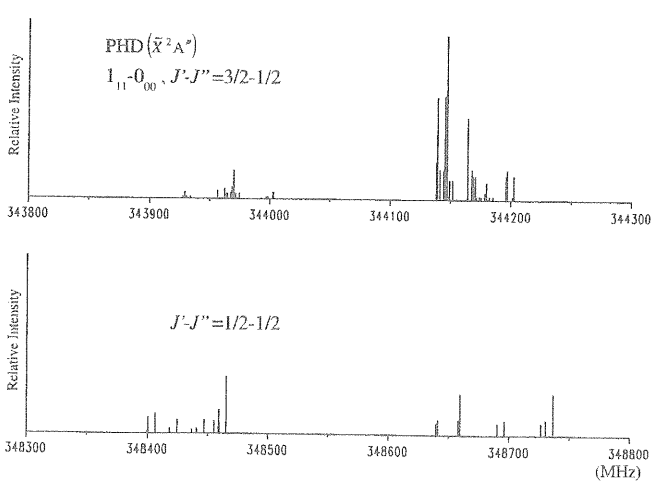

Fig. 1. A predicted stick diagram of the 1_{11}–0_{00} transition of PHD with calculated relative intensities.

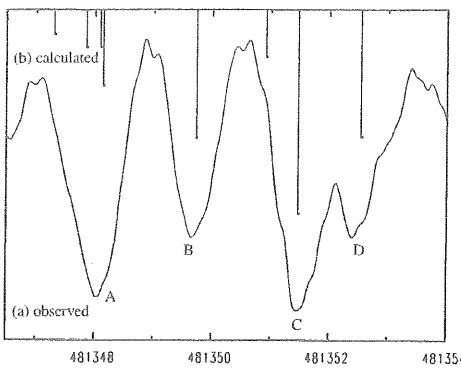

Fig. 2. An example of the hyperfine structure of the 2_{11}–1_{10}, $J = 3/2$–$1/2$, $F_1 = 2$–1 transition of PHD. The hyperfine components due to H and D overlap each other. The radical was produced by a 200 mA dc glow discharge in a mixture of PH_3 (15 mTorr), and D_2 (15 mTorr). The integration time was 20 s. (A) Composed of 4 components whose calculated relative intensities are depicted as vertical lines, from low to high frequency: ($F_2 = 5/2$–$3/2$, $F = 5/2$–$5/2$), ($F_2 = 3/2$–$1/2$, $F = 3/2$–$3/2$), ($F_2 = 3/2$–$1/2$, $F = 1/2$–$1/2$), and ($F_2 = 5/2$–$3/2$, $F = 3/2$–$1/2$). (B) ($F_2 = 5/2$–$3/2$, $F = 5/2$–$3/2$). (C) ($F_2 = 5/2$–$3/2$, $F = 5/2$–$5/2$) and ($F_2 = 3/2$–$1/2$, $F = 3/2$–$1/2$). (D) ($F_2 = 3/2$–$1/2$, $F = 5/2$–$3/2$).

portant R-branch transition, 1_{11}–0_{00}, was then detected in the same region of 300 GHz. Several b-type rotational transitions were successively measured. When a set of reasonable molecular constants were obtained from the observed line frequencies of these b-type transitions by a least-squares analysis, it was easy to identify and assign the weaker a-type R-branch transitions. Twenty-six rotational transitions, including 6 a-type and 20 b-type, were measured in the frequency region of 170–670 GHz. The hyperfine structure due to the deuterium nucleus was only resolved for the lowest N transitions, 1_{11}–0_{00}, 1_{10}–1_{01} and low F_2 components of $N = 2$ transitions. A typical example of the observed spectral pattern is shown in Fig. 2. A total of 219 spectral lines were measured, the observed frequencies of which are listed in Table 1.

3. Analysis

The measured line frequencies were analyzed using the following Hamiltonian for a doublet asymmetric top free radical bearing three nuclear spins,

$$H = H_{\rm rot} + H_{\rm sr} + H_{\rm hfs}({\rm P}) + H_{\rm hfs}({\rm H}) + H_{\rm hfs}({\rm D}), \qquad (1)$$

where $H_{\rm rot}$ is the rotational Hamiltonian with its centrifugal distortion effect using Watson's A-reduced form, $H_{\rm sr}$ the spin–rotation term with its centrifugal distortion effect, and $H_{\rm hfs}(i)$ the hyperfine structure term including Fermi contact, dipole–dipole, electric quadrupole (for deuterium), and nuclear spin–rotation interaction of the nucleus i. The matrix elements of the Hamiltonian were calculated using the standard method [14,15] with the basis $|NKSJI({\rm P})F_1I({\rm H})F_2I({\rm D})FM_F\rangle$ for which the following coupling scheme was applied:

$$\mathbf{J} = \mathbf{N} + \mathbf{S},\ \mathbf{F}_1 = \mathbf{J} + \mathbf{I}({\rm P}),$$
$$\mathbf{F}_2 = \mathbf{F}_1 + \mathbf{I}({\rm H}),\ \text{and}\ \mathbf{F} = \mathbf{F}_2 + \mathbf{I}({\rm D}). \qquad (2)$$

All the matrix elements of $\Delta\alpha = 0, \pm1, \pm2$ ($\alpha = N, J, F_1$, or F_2) were included. A least-squares fitting program was revised from the program used for the analysis of NHD [4] and the energy levels were calculated by direct diagonalization of the matrix.

The analysis of the observed spectral lines was not straightforward because the hyperfine structure due to the deuterium was resolved only for the two transitions, 1_{11}–0_{00} and 1_{10}–1_{01}, and the hyperfine components of larger N transitions were not resolved not only for the deuterium but also for the hydrogen atom. Therefore, a trial assignment was firstly made for the fine and phosphorus hyperfine components of a particular rotational transition on the basis of the predicted pattern and several relevant parameters were tentatively determined with other molecular constants fixed. When most of the main parameters of the rotational, centrifugal distortion, spin–rotation, and phosphorus hyperfine terms were determined, hydrogen hyperfine structure parameters were adjusted to get a more definite assignment of the observed spectral lines. This process was repeated to obtain an overall assignment which included the identification of very weak hyperfine structure components. Finally, 219 observed lines were assigned to the transitions of PHD, 145 of which were used in the final least-squares fitting analysis where the frequency of an unresolved line was compared with an averaged frequency of its component lines weighted by their calculated relative intensities. The standard deviation of the final fit is 58.7 kHz. Differences between observed and calculated frequencies of the 145 lines are within two standard deviations of the fit and are given in Table 1 and the 34 determined molecular constants are listed in Table 2. Electric quadrupole coupling constants of the deuterium, the nuclear spin–rotation coupling constants of H and D, and the off-diagonal components of magnetic dipole interaction for P, H, and D were included in the fit, but were not able to be determined. This is due to insufficient resolution of the deuterium hyperfine structure and relatively large separations between interacting levels related to $(\varepsilon_{ab} + \varepsilon_{ba})/2$ and T_{ab} for P, H, and D.

4. Results and discussion

Detailed molecular constants including the hyperfine coupling constants of P, H, and D were precisely determined for PHD in the present study. Most of the main molecular parameters were confirmed to be consistent

Table 1
Observed and calculated transition frequencies of the PHD radical (in MHz)[a]

N'–N''	J'–J'	F_1'–F_1''	F_2'–F_2''	F'–F''	ν_{obs}[b]	$\Delta\nu$[c]
1_{10}–1_{01}	3/2–3/2	2–2	5/2–5/2		171593.177(9)	0.027
			3/2–3/2	3/2–1/2		
			5/2–5/2	5/2–3/2	171589.233(20)	0.080
				5/2–7/2	171598.599(13)	0.076
				3/2–5/2	171596.938(11)	0.066
			3/2–3/2			
		1–1	3/2–3/2		171713.350(3)	−0.028
				5/2–3/2	171708.299(7)	0.061
			1/2–1/2	3/2–3/2	171717.236(21)	0.110
				1/2–1/2		
				3/2–1/2	171711.129(7)	0.050
				1/2–3/2	171723.355(22)	−0.091
			1/2–3/2	3/2–5/2	171745.678(15)	0.024
		2–1	5/2–3/2	7/2–5/2	171772.266(27)	−0.027
				3/2–3/2		
				3/2–1/2		
				5/2–3/2	171776.462(20)	0.320[d]
			3/2–1/2	5/2–3/2		
				3/2–1/2		
		1–2	3/2–5/2		171534.475(49)	0.192[d]
			1/2–3/2	1/2–1/2		
	3/2–1/2	2–1	5/2–3/2	7/2–5/2	169912.031(19)	−0.053
			3/2–1/2	5/2–3/2	169948.955(29)	−0.096
	1/2–1/2	1–1	3/2–3/2		176222.362(17)	−0.295[d]
			3/2–1/2	1/2–1/2	176225.822(132)	0.067
			1/2–3/2	3/2–5/2	176208.556(15)	0.056
				3/2–3/2	176210.018(34)	−0.003
				1/2–1/2		
			1/2–1/2	1/2–3/2		
		0–1	1/2–3/2	3/2–5/2	175865.681(4)	0.296[d]
	1/2–3/2	1–2	3/2–5/2	5/2–7/2	177903.861(18)	0.007
				3/2–5/2	177896.081(35)	0.007
			1/2–3/2	3/2–5/2	177860.808(29)	−0.077
		0–1	1/2–3/2	3/2–5/2	177725.740(35)	0.313[d]
2_{11}–2_{02}	5/2–5/2	3–3	7/2–7/2		227249.916(3)	0.009
			5/2–5/2		227250.909(8)	0.042
		2–2	5/2–5/2		227374.847(6)	−0.027
			3/2–3/2		227375.708(15)	0.020
	3/2–3/2	2–2			231181.372(6)	0.185[d]
			5/2–5/2	5/2–3/2	231183.885(23)	0.018
			3/2–3/2	3/2–1/2	231182.974(30)	0.313[d]
		1–1	3/2–3/2		230876.554(12)	0.205
			3/2–3/2	5/2–3/2	230879.801(22)	−0.183[d]
				3/2–1/2	230878.623(36)	−0.013
		1–2	3/2–5/2		231131.833(22)	0.411[d]
			1/2–3/2	1/2–1/2		
		2–1	5/2–3/2	7/2–5/2	230926.546(16)	0.317[d]
2_{02}–1_{11}	5/2–3/2	3–2	7/2–5/2		298912.203(8)	0.078
			5/2–3/2		298905.178(7)	−0.041
		2–1	5/2–3/2		298890.354(12)	0.036
			3/2–1/2	1/2–3/2		
				5/2–3/2	298882.895(10)	−0.018
				3/2–1/2		
	3/2–1/2	2–1	5/2–3/2	7/2–5/2	297137.152(14)	−0.061
			3/2–1/2	1/2–1/2		
				5/2–3/2	297133.958(28)	0.030
				5/2–5/2		
				3/2–1/2	297131.443(8)	−0.039
				3/2–3/2		
			3/2–1/2	5/2–3/2	297142.707(22)	−0.310[d]
			3/2–3/2	3/2–3/2	297121.277(9)	0.203[d]
		1–0	3/2–1/2	5/2–3/2		

Table 1 (*continued*)

N'–N''	J'–J'	F_1'–F_1''	F_2'–F_2''	F'–F''	ν_{obs}[b]	$\Delta\nu$[c]
3_{12}–3_{03}	7/2–7/2	4–4	9/2–9/2		325703.477(7)	0.003
			7/2–7/2			
		3–3	7/2–7/2		325848.935(6)	0.039
			5/2–5/2			
	5/2–5/2	3–3	7/2–7/2	9/2–9/2	330170.134(6)	−0.481[d]
			5/2–5/2	7/2–7/2		
				5/2–5/2		
			7/2–7/2	7/2–7/2	330169.221(17)	−0.004
				5/2–5/2		
			5/2–5/2	3/2–3/2		
		2–2	5/2–5/2	5/2–3/2	329895.038(12)	−0.096
				3/2–1/2		
				7/2–7/2	329893.672(4)	0.017
			3/2–3/2	5/2–5/2		
			5/2–5/2	5/2–5/2	329892.267(50)	0.004
				3/2–3/2		
			3/2–3/2	3/2–3/2		
				1/2–1/2		
1_{11}–0_{00}	3/2–1/2	2–1	5/2–3/2	7/2–5/2	344147.117(14)	0.060
			3/2–3/2	5/2–5/2	344179.726(6)	−0.064
			3/2–1/2	5/2–3/2	344139.315(5)	−0.011
				1/2–1/2	344141.421(11)	0.094
				3/2–3/2	344144.140(28)	0.270[d]
			5/2–3/2	5/2–3/2		
				3/2–1/2		
				5/2–5/2	344151.714(24)	−0.082
		1–0	3/2–1/2	5/2–3/2	344164.173(9)	0.051
				3/2–3/2	344168.788(31)	0.070
			1/2–1/2	3/2–3/2	344197.295(30)	0.217[d]
				3/2–1/2	344195.761(11)	−0.111
				1/2–3/2	344202.661(20)	0.033
		1–1	3/2–3/2	5/2–5/2	343969.823(31)	−0.054
	1/2–1/2	1–1	3/2–3/2	3/2–3/2	348458.535(14)	−0.430[d]
				1/2–3/2		
				5/2–3/2		
				5/2–5/2	348465.283(12)	0.056
				3/2–5/2		
			3/2–3/2	1/2–1/2	348454.929(21)	−0.012
				3/2–1/2		
			1/2–1/2	3/2–3/2	348406.101(30)	−0.088
				1/2–3/2		
				3/2–1/2	348400.249(11)	0.011
		1–0	3/2–1/2	5/2–3/2	348659.747(16)	0.299[d]
				3/2–3/2		
				3/2–1/2	348657.920(23)	−0.045
		0–1	1/2–3/2	3/2–3/2	348730.413(8)	−0.021
				1/2–3/2		
				1/2–1/2	348726.523(22)	−0.004
	3/2–1/2	1–0	3/2–1/2	3/2–1/2	344167.687(12)	0.175[d]
				1/2–1/2	344170.531(19)	0.079
		2–1	5/2–3/2	5/2–3/2	344145.632(9)	0.184[d]
				3/2–1/2		
			3/2–1/2	3/2–3/2		
		2–1	5/2–3/2	3/2–3/2	344149.065(27)	−0.177[d]
	1/2–1/2	0–1	1/2–3/2	3/2–5/2	348736.521(27)	0.036
		1–0	1/2–1/2	3/2–3/2	348641.254(14)	0.355[d]
				1/2–3/2		
3_{21}–3_{12}	7/2–7/2	4–4	9/2–9/2		367348.869(3)	−0.030
			7/2–7/2		367351.379(13)	0.057
		3–3	7/2–7/2		367367.585(5)	0.018
			5/2–5/2		367370.134(6)	0.074
	5/2–5/2	3–3	5/2–5/2	7/2–7/2	370515.838(8)	0.321[d]
		2–2	5/2–5/2		370489.870(8)	−0.163[d]

Table 1 (*continued*)

N'–N''	J'–J''	F_1'–F_1''	F_2'–F_2''	F'–F''	ν_{obs}[b]	$\Delta\nu$[c]
4_{22}–4_{13}	9/2–9/2	5–5	11/2–11/2		373751.349(10)	0.142[d]
			9/2–9/2		373752.782(8)	0.502[d]
		4–4	9/2–9/2		373790.697(71)	0.380[d]
			7/2–7/2		373791.810(9)	0.408[d]
	7/2–7/2	4–4	9/2–9/2		376645.211(8)	−0.001
			7/2–7/2		376643.286(11)	−0.041
		3–3	7/2–7/2		376582.327(19)	−0.057
			5/2–5/2		376580.473(11)	−0.138[d]
2_{12}–1_{11}	5/2–3/2	3–2	7/2–5/2		390598.777(23)	−0.006
			5/2–3/2	5/2–5/2		
			5/2–3/2		390593.788(33)	0.039
		2–1	5/2–3/2		390546.618(19)	0.020
			3/2–1/2	3/2–3/2		
			3/2–1/2		390541.235(28)	0.028
	3/2–1/2	2–1	5/2–3/2	7/2–5/2	389557.895(13)	−0.006
				5/2–3/2	389555.590(24)	0.086
				5/2–5/2		
			3/2–1/2	1/2–1/2		
				5/2–3/2	389559.733(22)	0.081
			5/2–3/2	3/2–1/2	389553.756(27)	−0.033
				3/2–3/2		
		1–0	3/2–1/2	5/2–3/2	389616.807(12)	0.179[d]
			1/2–1/2	3/2–3/2	389599.716(24)	0.309[d]
				3/2–1/2		
5_{23}–5_{14}	11/2–11/2	6–6			425482.782(26)	0.329[d]
		5–5			425548.372(25)	0.427[d]
	9/2–9/2	5–5			428750.713(14)	0.040
		4–4			428652.802(32)	0.006
2_{02}–1_{01}	5/2–3/2	3–2	7/2–5/2		425529.733(7)	−0.068
			5/2–3/2		425526.880(21)	−0.011
		2–1	5/2–3/2		425510.035(12)	0.013
			3/2–1/2	1/2–1/2		
				5/2–3/2	425507.376(43)	−0.083
	3/2–1/2	2–1	5/2–3/2	7/2–5/2	426392.476(23)	0.018
				5/2–3/2	426390.518(10)	−0.233[d]
				3/2–1/2		
			3/2–1/2	5/2–3/2	426384.189(25)	−0.035
				3/2–3/2	426380.485(23)	0.131[d]
				1/2–1/2		
			3/2–3/2	5/2–5/2		
				3/2–3/2	426377.630(30)	0.095
		1–0	3/2–1/2	5/2–3/2		
			1/2–1/2	3/2–1/2	426363.979(24)	0.036
				3/2–3/2		
4_{13}–4_{04}	9/2–9/2	5–5			472037.983(18)	−0.050
		4–4			472198.072(32)	−0.047
	7/2–7/2	3–3	7/2–7/2	9/2–9/2	477107.490(17)	0.096
				7/2–7/2		
			5/2–5/2	5/2–5/2		
				3/2–3/2		
		4–4	9/2–9/2	11/2–11/2	477367.291(26)	−0.596[d]
			7/2–7/2	7/2–7/2		
				5/2–5/2		
2_{11}–1_{10}	5/2–3/2	3–2	7/2–5/2		481186.538(25)	−0.019
			5/2–3/2	5/2–5/2		
			5/2–3/2		481181.025(30)	0.104
		2–1	5/2–3/2		481171.499(15)	−0.008
			3/2–1/2	3/2–3/2		
				5/2–3/2	481165.638(22)	0.065
				3/2–1/2		
				1/2–1/2	481168.664(22)	−0.013

Table 1 (*continued*)

N'–N''	J'–J'	F_1'–F_1''	F_2'–F_2''	F'–F''	ν_{obs}[b]	$\Delta\nu$[c]
		2–2	5/2–5/2		481112.103(28)	−0.502[d]
	3/2–1/2	2–1	5/2–3/2	7/2–5/2	481351.482(25)	0.078
			3/2–1/2	3/2–1/2		
			3/2–1/2	5/2–3/2	481352.469(39)	−0.057
			5/2–3/2	5/2–3/2	481349.695(13)	−0.050
				5/2–5/2	481347.958(14)	0.011
				3/2–1/2		
			3/2–1/2	3/2–3/2		
				1/2–1/2		
		1–0	3/2–1/2	5/2–3/2	481658.688(26)	0.037
				3/2–3/2	481655.163(49)	0.332[d]
				3/2–1/2		
				1/2–3/2	481651.954(12)	−0.063
				1/2–1/2		
			1/2–1/2	3/2–3/2	481643.845(14)	−0.265[d]
				1/2–3/2	481639.143(20)	−0.065
		1–1	3/2–3/2	5/3–5/3	481301.599(22)	0.327[d]
				3/2–1/2		
			1/2–1/2	3/2–3/2		
2_{21}–2_{12}	5/2–5/2	3–3	7/2–7/2		516127.230(11)	−0.071
		2–2	5/2–5/2		516281.871(29)	−0.069
			3/2–3/2		516286.546(25)	0.442[d]
	3/2–3/2	2–2	5/2–5/2		523704.790(24)	0.008
			3/2–3/2		523698.471(24)	−0.224[d]
				3/2–5/2	523696.034(44)	0.054
		1–1	3/2–3/2		523329.640(28)	−0.064
2_{12}–1_{01}	5/2–3/2	3–2	7/2–5/2	7/2–5/2	517216.176(28)	0.168[d]
				5/2–3/2		
			5/2–3/2	7/2–5/2		
			7/2–5/2	7/2–7/2	517221.057(34)	−0.048
			5/2–3/2	5/2–5/2		
		2–1	5/2–3/2		517166.067(34)	−0.022
			3/2–1/2	5/2–3/2		
	3/2–1/2	2–1	5/2–3/2	7/2–5/2	518813.006(13)	−0.141[d]
				3/2–1/2		
				5/2–5/2	518810.005(45)	−0.466[d]
			3/2–1/2	3/2–3/2	518798.184(25)	−0.241[d]
				1/2–1/2		
		1–0	3/2–1/2	5/2–3/2	518873.006(25)	−0.060
				3/2–3/2	518870.294(18)	−0.235[d]
				3/2–1/2		
				1/2–1/2	518868.636(20)	−0.275[d]
			1/2–1/2	3/2–3/2	518855.867(24)	−0.020
				3/2–1/2		
				1/2–3/2	518852.411(53)	−0.241[d]
				1/2–1/2		
		1–1	3/2–3/2	5/2–5/2	519143.100(12)	−0.029
				1/2–1/2		
3_{03}–2_{12}	7/2–5/2	4–3	9/2–7/2		524381.371(16)	0.264[d]
			7/2–5/2		524378.248(25)	0.112
		3–2	7/2–5/2		524379.539(48)	−0.044
			5/2–3/2		524376.474(27)	−0.014
	5/2–3/2	3–2	7/2–5/2	9/2–7/2	524135.008(20)	−0.057
			5/2–3/2	5/2–3/2		
		2–1	5/2–3/2	7/2–5/2	524102.264(30)	0.244[d]
			3/2–1/2	5/2–3/2		
				3/2–1/2		
6_{24}–6_{15}	13/2–13/2	7–7			531987.893(14)	0.016
		6–6			532078.527(16)	0.164[d]
	11/2–11/2	6–6			536015.364(11)	−0.519[d]
		5–5			535888.361(19)	−0.031

Table 1 (*continued*)

N'–N''	J'–J'	F_1'–F_1''	F_2'–F_2''	F'–F''	ν_{obs}[b]	$\Delta\nu$[c]
7_{34}–7_{25}	15/2–15/2	8–8			555150.559(10)	−0.045
		7–7			555172.713(12)	0.010
	13/2–13/2	7–7			557660.034(13)	0.062
		6–6			557629.727(24)	0.006
3_{13}–2_{12}	7/2–5/2	4–3	9/2–7/2		579850.742(26)	0.308[d]
			7/2–5/2		579848.256(21)	−0.132[d]
		3–2	7/2–5/2		579822.955(23)	0.342[d]
	5/2–3/2	3–2	7/2–5/2		579737.094(26)	−0.186[d]
			5/2–3/2			
		2–1	5/2–3/2		579746.896(15)	−0.038
			3/2–1/2	5/2–3/2		
				3/2–1/2		
6_{33}–6_{24}	13/2–13/2	7–7	15/2–15/2		558817.821(21)	0.018
		6–6	13/2–13/2			
		7–7	13/2–13/2		558819.312(20)	0.141[d]
		6–6	11/2–11/2			
	11/2–11/2	6–6	13/2–13/2		561179.978(15)	0.058
		5–5	11/2–11/2			
		6–6	11/2–11/2		561177.966(22)	−0.106
		5–5	9/2–9/2			
3_{22}–3_{13}	7/2–7/2	4–4	9/2–9/2		590058.517(15)	−0.203[d]
			7/2–7/2		590060.685(26)	−0.012
		3–3	7/2–7/2		590196.097(22)	−0.276[d]
			5/2–5/2		590198.230(15)	0.013
	5/2–5/2	3–3	7/2–7/2		596532.803(9)	0.234[d]
			5/2–5/2		596529.677(23)	0.013
		2–2	5/2–5/2		596277.910(16)	0.210[d]
			3/2–3/2		596274.709(23)	0.017
5_{32}–5_{23}	11/2–11/2	6–6	13/2–13/2		601818.060(16)	−0.023
			11/2–11/2		601820.597(12)	0.295[d]
		5–5	11/2–11/2		601805.740(26)	−0.016
			9/2–9/2		601808.447(19)	0.444[d]
	9/2–9/2	5–5	11/2–11/2		604632.056(29)	0.356[d]
			9/2–9/2		604628.567(29)	0.016
		4–4	9/2–9/2		604650.253(22)	−0.008
			7/2–7/2		604646.925(29)	−0.203[d]
8_{35}–8_{26}	17/2–17/2	9–9			607715.245(20)	−0.021
		8–8			607762.141(14)	0.019
	15/2–15/2	8–8			610805.897(29)	−0.070
		7–7			610744.442(12)	0.064
3_{03}–2_{02}	7/2–5/2	4–3	9/2–7/2		616067.898(43)	0.145[d]
		3–2	7/2–5/2		616035.607(28)	−0.060
	5/2–3/2	3–2	7/2–5/2		616556.183(28)	0.393[d]
			5/2–3/2		616552.518(31)	0.092
		2–1	5/2–3/2		616597.802(15)	0.721[d]
3_{22}–2_{21}	7/2–5/2	4–3	9/2–7/2		653781.813(13)	−0.044
			7/2–5/2		653777.505(11)	−0.032
		3–2	7/2–5/2		653737.038(10)	−0.017
			5/2–3/2		653732.758(22)	0.081
	5/2–3/2	3–2	7/2–5/2	9/2–7/2	652565.854(31)	−0.487[d]
			5/2–3/2	3/2–1/2		
				7/2–5/2	652568.453(37)	0.135[d]
		2–1	5/2–3/2	7/2–5/2	652695.273(24)	−0.616[d]
			3/2–1/2	5/2–3/2	652698.142(20)	0.022
5_{14}–5_{05}	11/2–11/2	6–6			656176.957(12)	0.035
		5–5			656337.478(24)	0.729[d]
		4–4	9/2–9/2	11/2–11/2	662028.422(28)	−0.031
				9/2–9/2		
			7/2–7/2	7/2–7/2		

Table 1 (*continued*)

N'–N''	J'–J'	F_1'–F_1''	F_2'–F_2''	F'–F''	ν_{obs}[b]	$\Delta\nu$[c]
				5/2–5/2		
4_{31}–4_{22}	9/2–9/2	5–5	11/2–11/2		659537.878(12)	0.019
			9/2–9/2		659541.345(13)	0.257[d]
		4–4	9/2–9/2		659532.606(28)	0.023
			7/2–7/2		659535.864(28)	0.005

[a] Standard deviation of the fit is 58.7 kHz. Calculated frequencies were obtained from the molecular constants given in Table 2.
[b] Values in parentheses indicate the variances of the measured frequency in units of the last significant digits.
[c] Residuals in least-squares fit. $\Delta\nu = \nu_{obs} - \nu_{calc}$.
[d] Not included in the least-squares fit.

Table 2
Molecular constants of PHD ($\tilde{X}^2A''$) (in MHz)[a]

Rotation and centrifugal distortion constants		Fine and hyperfine coupling constants	
A	259409.834(39)	ε_{aa}	−5881.927(87)
B	131908.017(46)	ε_{bb}	−2394.875(77)
C	86217.514(45)	ε_{cc}	−4.937(69)
		$\lvert(\varepsilon_{ab}+\varepsilon_{ba})/2\rvert$	1773.0(32)
Δ_N	2.3459(84)		
Δ_{NK}	23.2412(115)	Δ_N^S	0.1375(58)
Δ_K	−8.5825(155)	Δ_{KN}^S	1.2142(163)
δ_N	0.76036(71)	Δ_K^S	0.602(36)
δ_K	15.8791(124)	δ_N^S	0.06438(119)
		δ_K^S	0.9454(143)
Φ_N	−0.00046(43)		
Φ_{NK}	0.00702(50)	a_F (P)	207.771(120)
Φ_{KN}	−0.00704(115)	T_{aa} (P)	−308.426(123)
ϕ_{NK}	0.00602(24)	T_{bb} (P)	−313.698(151)
ϕ_K	0.0081(33)	$\lvert T_{ab}(\mathrm{P})\rvert$[b]	10.62(fixed)
		C_{aa}(P)	0.760(64)
		C_{bb}(P)	0.450(51)
		C_{cc}(P)	0.048(44)
		a_F(H)	−48.774(94)
		T_{aa}(H)	−17.418(166)
		T_{bb}(H)	12.236(185)
		$\lvert T_{ab}(\mathrm{H})\rvert$[b]	5.023(fixed)
		a_F(D)	−7.447(59)
		T_{aa}(D)	2.005(109)
		T_{bb}(D)	−2.977(137)
		$\lvert T_{ab}(\mathrm{D})\rvert$[b]	−0.3(fixed)

[a] Values in parentheses indicate three standard deviations in units of the last significant digits.
[b] Relative sign of $|T_{ab}(\mathrm{P})|$ and $|T_{ab}(\mathrm{H})|$ to $|(\varepsilon_{ab}+\varepsilon_{ba})/2|$ was calculated to be the same and that of $|T_{ab}(\mathrm{D})|$ to be the opposite.

with the predicted constants estimated from those of the parent molecule PH_2 and the doubly deuterated species PD_2 by a principal axis rotation of 38.74°. Furthermore, most of the main molecular constants of the parent and doubly deuterated species have been discussed in previous studies which focused on the molecular structure and harmonic force field [9], spin–rotation [16], Renner–Teller effect [17], spin density [6,18], and detectability in space [8].

Since the off-diagonal components of the magnetic dipole coupling constant for H and D can now be derived from the results of the present study, it is worthwhile to discuss the principal values and axes of the magnetic dipole tensor in PH_2. If the magnetic dipole interaction does not change significantly upon deuterium substitution in PH_2, the observed hyperfine coupling constants of PHD can relate to those of PH_2 via a principal axis rotation angle, where the only unknown parameter is T_{ab} of PH_2. From the observed diagonal components of both the PH_2 and PHD species, T_{ab} for PH_2 was determined to be 15.57 MHz and one of the principal axes, denoted as the σ-axis for the hydrogen magnetic dipole tensor in PH_2 made an angle of 2.29° with the HP bond. The principal value along the σ-axis, T_σ, was then calculated as 12.93 MHz and its perpendicular component $T_\perp$ as −18.39 MHz. A similar calculation was made for the deuterium in PD_2 and PHD; T_{ab} for PD_2 was found to be 2.50 MHz, and T_σ, 2.09 MHz with an angle of 2.02°. These results show that T_σ is almost parallel with the PH or PD chemical bond.

Similarly, from the hyperfine coupling constants of NH_2 [1] and NHD [4] the T_σ for NH_2 was calculated to be 58.57 MHz with an angle of 1.68° with the NH bond. If T_σ of XH_2 is due to an unpaired electron near the X atom, T_σ(H) is therefore considered to be proportional to $\rho_\pi\langle 1/r^3\rangle$, where ρ_π is π electron spin density near the X atom and r is the XH bond length. The ρ_π of PH_2 and NH_2 was estimated to be 0.848 and 0.788 respectively [19]. Hirao et al. [9] derived the r_z bond length of PH for PH_2 to be 1.43365(23) Å and that of PD for PD_2 to be 1.42852(17) Å. The equilibrium bond length of PH was calculated to be 1.41543(85) Å simply from the r_z bond lengths of PH and PD [20]. When these values were combined with the r_e of 1.02541(120) Å for NH in NH_2 [4], the ratio of $\rho_\pi\langle 1/r^3\rangle$ between the PH of PH_2 and NH of NH_2 was calculated to be 2.44, which significantly differs from the ratio of T_σ for PH of PH_2 and NH of NH_2, i.e., 4.53. This means that the distribution of unpaired electrons around PH and NH cannot be explained by a simple unpaired electron distribution model [3]. The present result should provide a good challenge to modern sophisticated quantum mechanical calculation as until now, anisotropic hyperfine coupling constants of PH_2 and NH_2 have been relatively poorly estimated [21,22].

Acknowledgments

The authors thank I.K. Ahmad for her critical reading of the manuscript. The present study was supported by Grants-in-Aid from the Ministry of Education, Science, and Culture (No. 12440161).

References

[1] M. Tonooka, S. Yamamoto, K. Kobayashi, S. Saito, J. Chem. Phys. 106 (1997) 2563–2568.
[2] M. Kanada, S. Yamamoto, S. Saito, J. Chem. Phys. 94 (1991) 3423–3428.
[3] T.C. Steimle, J.M. Brown, R.F. Curl Jr., J. Chem. Phys. 73 (1980) 2552–2558.
[4] K. Kobayashi, H. Ozeki, S. Saito, M. Tonooka, S. Yamamoto, J. Chem. Phys. 107 (1997) 9289–9296.
[5] S. Saito, Y. Endo, E. Hirota, J. Mol. Spectrosc. 98 (1983) 138–145.
[6] Y. Endo, S. Saito, E. Hirota, J. Mol. Spectrosc. 97 (1983) 204–212.
[7] M. Kajita, Y. Endo, E. Hirota, J. Mol. Spectrosc. 124 (1987) 66–71.
[8] L. Margulès, E. Herbst, V. Ahrens, F. Lewen, G. Winnewisser, H.S.P. Müller, J. Mol. Spectrosc. 211 (2002) 211–220.
[9] T. Hirao, S. Hayakashi, S. Yamamoto, S. Saito, J. Mol. Spectrosc. 187 (1998) 153–162.
[10] H. Guenebaut, B. Pascat, C. R. Acad. Sci. Paris 259 (1964) 2412–2415.
[11] H. Guenebaut, B. Pascat, J.M. Berthou, J. Chim. Phys. 62 (1965) 867–877.
[12] S. Saito, M. Goto, Astrophys. J. 410 (1993) L53–L55.
[13] P. Helminger, R.L. Cook, F.C. De Lucia, J. Mol. Spectrosc. 40 (1971) 125–136.
[14] I.C. Bowater, J.M. Brown, A. Carrington, Proc. R. Soc. London Ser. A 333 (1973) 265–288.
[15] A.R. Edmonds, Angular Momentum in Quantum Mechanics, Princeton University Press, Princeton, NJ, 1957.
[16] R.N. Dixon, G. Duxbury, D.A. Ramsay, Proc. R. Soc. London A 296 (1967) 137–160.
[17] T. Barrow, R.N. Dixon, G. Duxbury, Mol. Phys. 27 (1974) 1217–1234.
[18] P.B. Davies, D.K. Russell, B.A. Thrush, H.E. Radford, Chem. Phys. 44 (1979) 421–426.
[19] S. Saito, Y. Endo, E. Hirota, J. Chem. Phys. 85 (1986) 1778–1784.
[20] T. Oka, Y. Morino, J. Mol. Spectrosc. 8 (1962) 300–314.
[21] M.T. Nguyen, S. Creve, L.A. Eriksson, L.G. Vanquickenborne, Mol. Phys. 91 (1997) 537–550.
[22] M.A. Austen, L.A. Eriksson, R.L. Boyd, Can. J. Chem. 72 (1994) 695–704.